Received September 8, 2017; Accepted January 25, 2018 Kogaku **47**, 4 (2018) 165–173

Simultaneous Measurement of Transparent Plate Surface Topography and Thickness Variation Using Arbitrary Wavelength Shifting Interferometry

Katsuichi KITAGAWA* and Jun MIZOJIRI**

*Independent Consultant, 241-41 Fuke-cho, Moriyama-shi, Shiga, 524-0033
**Mizojiri Optical Co., Ltd., 2-8-2 Nishishinagawa, Shinagawa-ku, Tokyo, 141-003

Wavelength scanning interferometry is a known technique to precisely measure the surface topography and plate thickness for transparent materials, such as glass. However, conventional methods have some problems in the practical applications that they require precise sample surface position adjustments relative to the reference surface, and highly accurate linear wavelength scanning. We propose a least- squares model-fitting algorithm which estimates the surface topography and plate thickness from the interferograms obtained by arbitrary wavelength shift. The LD wavelength tuned by temperature control is measured by a wavelength meter, and the measured values are used in the data analysis. The validity of the proposed method is proved by computer simulations and actual experiments. The atual test results showed good agreement with those by a conventional method, and a one-sigma repeatability of 2 nm was obtained.

Key words: wavelength-shifting interferometry, transparent plate, topography, thickness measurement, model-fitting

1. Introduction

Wavelength scanning interferometry [1-4] (WSI; also called wavelength shift interferometry) is known as a method for three-dimensionally measuring the surface profile and the plate thickness of transparent objects such as glass plates with high accuracy. WSI uses a wavelength tunable laser as the light source to scan the wavelength linearly in time, and can measure the distance to each interface by separating the superimposed interference signal from the interfaces using the fact that the frequency of the intensity signal obtained is proportional to the optical distance.

As a measurement algorithm for transparent objects by WSI, a model fitting method [5-7] that finds unknown variables including the phases by fitting the model expression representing the interference light intensity and the observed intensity waveform (interferogram) by least squares, the extended PSI method [8-13] which is an extension of the phase shifting (PSI) method typified by the 4-point method and the 5-point method, and the Fourier transform method [14-17] which calculate the phase at each frequency by the Fourier transform.

However, in the extended PSI method and the Fourier transform method, it is necessary to strictly adjust the distance between the reference surface and the sample surface so that the frequency of the superimposed sine waves have an integer ratio. A common problem with WSI is that highly accurate wavelength scanning (or wavelength shift at constant intervals) is required, and its nonlinearity is a major cause of measurement error. The required wavelength scanning accuracy is on the order of 1 pm because the total scanning wavelength range is about 0.1 nm, but the resolution of wavelength scanning lasers available for industrial use is about 10 pm. There is no product that meets the required accuracy.

Wavelength scanning non-linearity problems is also an important issue in the optical frequency domain refectometry (OFDR) [18], and some methods of solving it by using an external wavelength meter or a reference interferometer has been proposed. The first method is a method of feedback controlling the laser wavelength based on wavemeter data [19]. The second method is to control the imaging timing of the camera by the output of the wavemeter [20]. The third method is to resample the intensiy signal data using wavelength data [21]. However, all of them require the development of control systems or signal processing algorithms, and lack versatility.

On the other hand, in the PSI method, there is a proposa [l5, 22-25] that estimates the shift amounts as an unknown variables by the least-squares method in order to allow the variation of the phase shift amounts. However, they target opaque objects whose model is rather simple. On the other hand, in the case of the transparent object, the optics is three-beam interference, and the model formula contains three periodic functions. For this reason, it becomes an optimization problem of a multimodal solution space where there are many unknown variables and the local solutions are distributed in a complicated manner, and it is expected to be of poor practicality.

To solve the above problem, the authors propose an arbitrary wavelength shifting interferometry (called AWSI method) [26]. In this method, the measured values of wavelength by a wavemeter are directly used for least-squares fitting to estimate the surface profile, back surface profile, and plate thickness distribution.

This eliminates the need for wavelength scanning accuracy and allows arbitrary wavelength shifts. In this paper, we report the proposed method and the experimental results using a computer and an actual sample. As far as the authors are aware, no research has been reported so far that the wavelength shift amount in the WSI method is arbitrarily determined by using the wavelength measurement value obtained by the wavelength meter.

E-mail: katsuichi.kitagawa@nifty.com

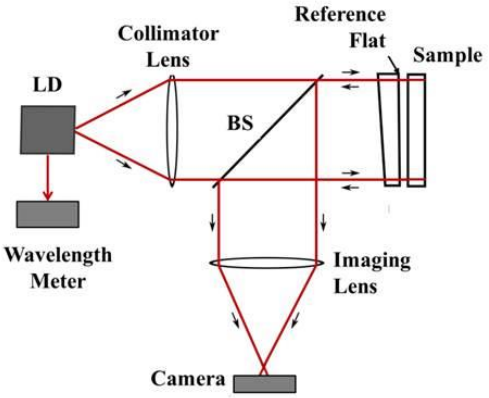

Fig. 1 Setup for Fizeau interferometer with a wavelength tunable laser.

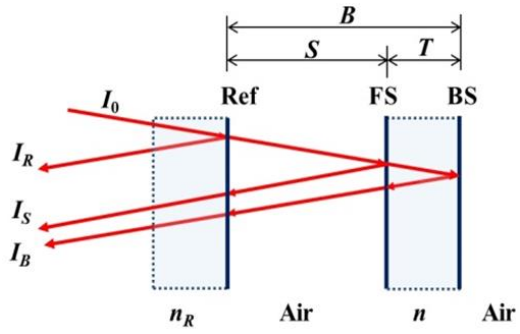

Fig. 2 Schematic of 3-beam interference in the Fizeau interferometer.

2. Measurement principle

2.1 Basic algorithm

A Fizeau interferometer is constructed as shown in Fig. 1. A wavelength tunable laser is used as the light source, and it is possible to shift to any wavelength. The shifted wavelength is measured with a high precision wavelength meter. If the sample is transparent, there are three reflecting surfaces, making three-beam interference, and the interference image will be a superimposed image from (1) reference surface and sample surface, (2) reference surface and sample back surface, and (3) sample surface and back surface (See Fig. 6 below). The main purpose of this research is to develop an algorithm for separating these three signals using the arbitrary shifted wavelengths.

In the Fizeau interferometer shown in Fig. 2, the reference surface Ref, the front surface FS, and the back surface BS are arranged in this order, and the optical distances between Ref-FS, Ref-BS, and FS-BS are *S*, *B*, and *T*, respectively. Then, the observed intensity *I* is expressed as the following equation, taking into account the phase inversion of Ref-FS interference and FS-BS interference:

$$I = I_S + I_B + I_R - 2\sqrt{I_S I_R}\cos(4\pi S/\lambda) + 2\sqrt{I_B I_R}\cos(4\pi B/\lambda) - 2\sqrt{I_S I_B}\cos(4\pi T/\lambda) \quad (1)$$

where I_S, I_B, I_R are the intensities of reflected light at each interface.

Note that the multiple reflected lights of the second and subsequent orders are ignored in Fig. 2. This validity is briefly supplemented. The secondary reflected light undergoes interface reflection twice more than the primary reflected light. Since the interface reflectance is about 4% for glass, the amount of secondary reflected light is less than 0.2% of the amount of primary reflected light. Since the interference amplitude is proportional to the square root of the product of the amounts of light, the interference amplitude of secondary reflected light is about 4% of the primary light. Although it may depend on other conditions, it is expected that the influence of this interference component on the measurement result is usually minimized by the least-squares fit, and eventually can be ignored.

If we try to fit the Eq. (1) as a model to the observed intensity data with wavelength shift, using $T = B - S$, there are five unknown variables I_S, I_B, I_R, S and B.

By the way, this model function is the sum of three periodic functions, and the least-squares fit is an ill-posed optimization problem with a complex multimodal solution space. Therefore, the unknown variable is reduced by setting the refractive index of air to 1 and making the reference plate refractive index n_R and the sample refractive index n to be known. In Fig. 2, the interface reflectances *RR*, *RS*, and *RB* on the Ref, FS, and BS surfaces respectively are given by:

$$R_R = \{(n_R - 1)/(n_R + 1)\}^2 \quad (2)$$

$$R_S = R_B = \{(n - 1)/(n + 1)\}^2 \quad (3)$$

Also, letting I_0 be the incident light intensity on the reference surface, the intensities of reflected light I_S, I_B, I_R are expressed by:

$$I_R = I_0 R_R \quad (4)$$

$$I_S = I_0(1 - R_R)^2 R_S \quad (5)$$

$$I_B = I_0(1 - R_R)^2 R_S(1 - R_S)^2 \quad (6)$$

Using Eqs.(4)-(6), Eq(1) holds:

$$I = I_0\,[a - b_S\cos(4\pi S/\lambda) + b_B\cos(4\pi B/\lambda) - b_T\cos\{4\pi(B - S)/\lambda\}] \quad (7)$$

where, using Eqs.(4)-(6), *a*, b_S, b_B, b_T are expressed:

$$a = (I_S + I_B + I_T)/I_0 = R_R + (1 - R_R)^2 R_S + (1 - R_R)^2 R_S(1 - R_S)^2 \quad (8)$$

$$b_S = 2\sqrt{I_R I_S}/I_0 = 2(1 - R_R)\sqrt{R_R R_S} \quad (9)$$

$$b_B = 2\sqrt{I_R I_B}/I_0 = 2(1 - R_R)(1 - R_B)\sqrt{R_R R_B} \quad (10)$$

$$b_T = 2\sqrt{I_S I_B}/I_0 = 2(1 - R_R)^2(1 - R_S)R_S \quad (11)$$

Note that these are known variables obtained by the refractive index and Eq.(2) and (3). Therefore, the model formula is as shown in Eq. (7), and the unknown variables are reduced to I_0, *S* and *B*. The incident light intensity I_0 is a device constant that depends on the illumination, and *S* and *B* are the value to be measured, so the three unknown variables can be said to be the theoretical lower limits. In addition, reduction of unknown variables is effective not only for stabilizing least-squares fitting (by local solution avoidance), but also for reducing computational cost.

Next, consider the wavelength shift method. The method is to obtain the unknown variables I_0, *S*, *B* by changing the wavelength and observing the intensity in Eq. (7). However, finding the absolute values of *S* and *B* is extremely difficult in practice because the the interference signal is periodic and the interference orders are unknown. Therefore, as in ordinary phase-shifting interferometry, the fractional components below 2π of the phase of *S*, *B* at the initial wavelength λ_0 are defined as unknown variables ϕ_{S0} and ϕ_{B0}.

If the wavelength shift amount is $\Delta\lambda_i$ (i = 1, 2,…, m), the i-th wavelength is $\lambda_i = \lambda_0 + \Delta\lambda_i$. The phase ϕ_{Si} of the distance *S* at this wavelength is $\phi_{Si} = 4\pi S/\lambda_i$, and the amount of phase shift from the initial phase is $\Delta\phi_{Si} = -4\pi S(\Delta\lambda_i)/\lambda_i\lambda_0$.

That is, the amount of phase shift depends on the distance *S*, which is an unknown variable to be measured. Therefore, using the estimated value S_0 of the unknown variable *S*, the phase shift amount is

$$\Delta\phi_{Si} = -4\pi S_0(\Delta\lambda_i)/\lambda_i\lambda_0 \quad (12)$$

Similarly, using the estimated value B_0 of the unknown variable *B*,

$$\Delta\phi_{Bi} = -4\pi B_0(\Delta\lambda_i)/\lambda_i\lambda_0 \quad (13)$$

$$\Delta\phi_{Ti} = -4\pi(B_0 - S_0)(\Delta\lambda_i)/\lambda_i\lambda_0 \quad (14)$$

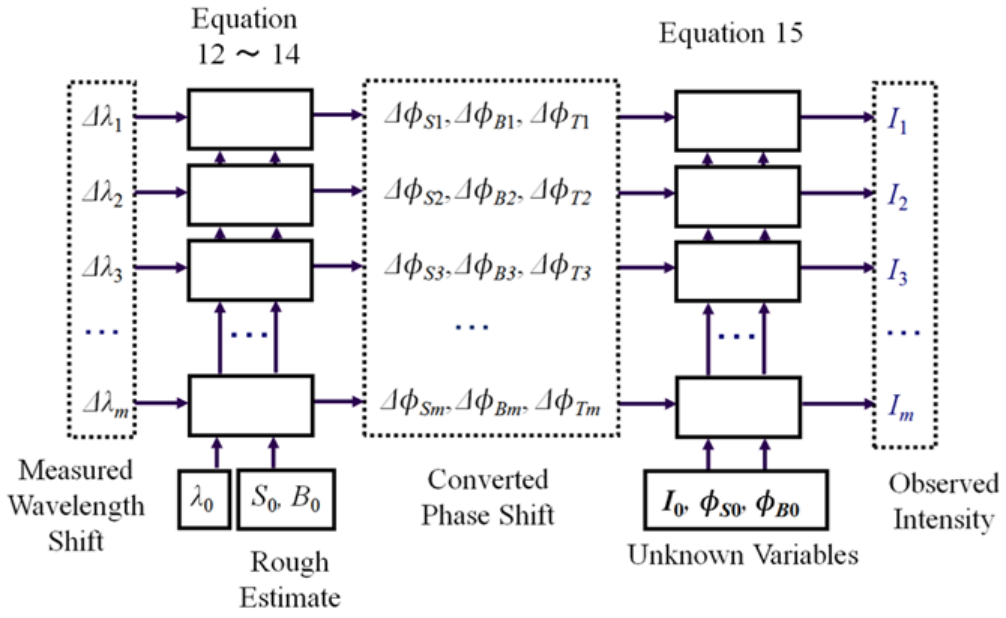

Fig.3 Schematic of data processing for arbitrary wavelength shifting algorithm

That is, Eqs. (12)-(14) are conversion formulas from the wavelength shift amount to the phase shift amount. As a result of considering the effect of the error of the estimated values, it is judged that the effect is very small and can be ignored in practice (see Supplement 1).

Therefore, the model equation when the wavelength λ is shifted from the initial value λ_0 by $\Delta\lambda_i$ is obtained by modifying Eq. (7):

$$I(i) = I_0\,[a - b_s\cos(\phi_{S0} + \Delta\phi_{Si}) + b_B\cos(\phi_{B0} + \Delta\phi_{Bi}) - b_T\cos\{(\phi_{B0} - \phi_{S0}) + (\Delta\phi_{Bi} - \Delta\phi_{Si})\}] \quad (15)$$

The unknown variables in this model equation are the incident light intensity I_0, and two phases ϕ_{S0}, ϕ_{B0}, which can be estimated by the least-squares fitting between the observed values I_i and the model:

$$SSE(I_0, \phi_{S0}, \phi_{B0}) \equiv \sum_{i=1}^{m}[I_i - I(i)]^2 = \min \quad (16)$$

The necessary condition for solving this least-squares fitting problem is m>=3.

This least-squares fit is non-linear, and the computational cost is high in ordinary iterative optimization methods. Therefore, the linearization described below is used to speed up the calculatiom.

The model equation (15) is transformed by using the addition theorem and variable transform of $C_S = I_0\cos\phi_{S0}$, $S_S = I_0\sin\phi_{S0}$, $C_B = I_0\cos\phi_{B0}$, $S_B = I_0\sin\phi_{B0}$, $C_T = I_0\cos\phi_{T0}$, $S_T = I_0\sin\phi_{T0}$. Then Eqs.(15)(16) become a linear least squres problem:

$$I(i) = aI_0 - b_s\cos(\Delta\phi_{Si})\,C_S + b_s\sin(\Delta\phi_{Si})\,S_S + b_B\cos(\Delta\phi_{Bi})\,C_B - b_B\sin(\Delta\phi_{Bi})\,S_B - b_T\cos(\Delta\phi_{Ti})\,C_T + b_T\sin(\Delta\phi_{Ti})\,S_T \quad (17)$$

$$SSE(I_0, C_S, S_S, C_B, S_B, C_T, S_T) \equiv \sum_{i=1}^{m}[I_i - I(i)]^2 = \min \quad (18)$$

This problem has seven unknowns, I_0, C_S, S_S, C_B, S_B, C_T, S_T, and can be solved analytically as a simultaneous linear equations with 7 unknown variables (see Supplement 2).

From the solution, we can obtain the relative phases by $\phi_{S0} = \mathrm{atan}(S_S/C_S)$, $\phi_{B0} = \mathrm{atan}(S_B/C_B)$, $\phi_{T0} = \mathrm{atan}\,(S_T/C_T)$.

The measurement principle of AWSI method described above is illustrated in Fig. 3. The left half is the phase shift amount calculation block from the measured wavelength values and the estimated values of S and B, and the right half represents an inverse problem that estimates three unknown variables (incident light intensity I_0, phases ϕ_{S0}, ϕ_{B0}) from the phase shift amounts that are the input of the model equation (15) and the observed intensity values that are the output of the equation.

From the obtained front surface phase ϕ_{S0} and back surface phase ϕ_{B0}, the relative and physical front and back surface height variations $\Delta S'$, $\Delta B'$ and plate thickness variation $\Delta T'$ are obtained by the following procedure:

(1) Obtain the surface phase Φ_{S0} by unwrapping the surface phase.
(2) Surface height variation $\Delta S = (\Phi_{S0}/2\pi)(\lambda_0/2)$.
(3) Surface height variation from the sample side $\Delta S' = -\Delta S$.
(4) Obtain the thickness phase Φ_{T0} by unwrapping the thickness phase $(\phi_{B0} - \phi_{S0})$.
(5) Physical thickness variation $\Delta T' = (\Phi_{T0}/2\pi)(\lambda_0/2)/n$.
(6) Physical backside height variation $\Delta B' = \Delta S + \Delta T'$.

3. Computer experiment

3.1 Experimental method

A theoretical waveform was created under the following conditions: (1) Initial wavelength λ_0= 600 nm; (2) Wavelength shift amount $\Delta\lambda_i = 0.2(i-1)^2/99^2$; (3) Number of shifts m = 100; (4) Incident light intensity I_0 = 100; (5) Surface distance S = 10 mm; (6) Physical plate thickness T'= 10 mm; (7) Reference plate refractive index n_R = 1.46; (8) Sample refractive index n = 1.46; (9) Backside distance B = 24.6 mm.

In order to emphasize the non-linearity of the wavelength shift, a quadratic change in the range of 0 to 0.2 nm was assumed, as shown by the dotted line in Fig. 4. The obtained waveform is shown by the solid line in Fig. 4. The estimated values S_0, and B_0 required for conversion from the wavelength shift amount to the phase shift amount were set to the true values.

3.2 Experimental results

The fitting results are shown in Table 1 and Fig. 5(a). The intensity of incident light and the front and back surface phases are correctly estimated. Also, the signal waveforms of the front surface, the back surface, and the film thickness that have been extracted are shown in Fig. 5(b)(c)(d). It was also confirmed that the true values can be stably obtained even if ±5% random noise is added to the intensity data.

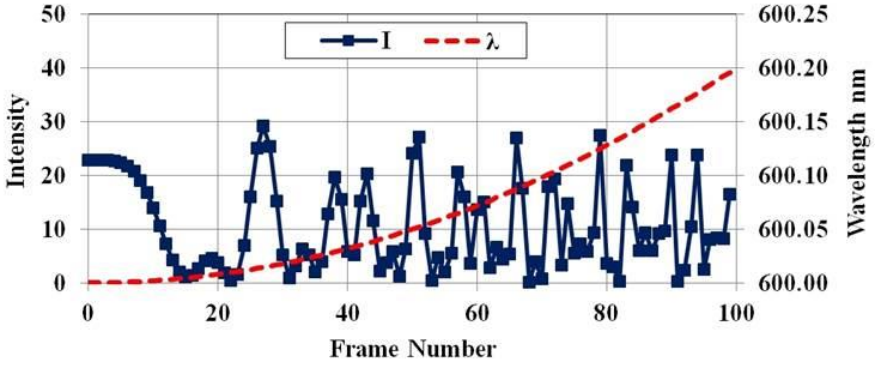

Fig.4 Simulated interferogram and wavelength change corresponding to frame number.

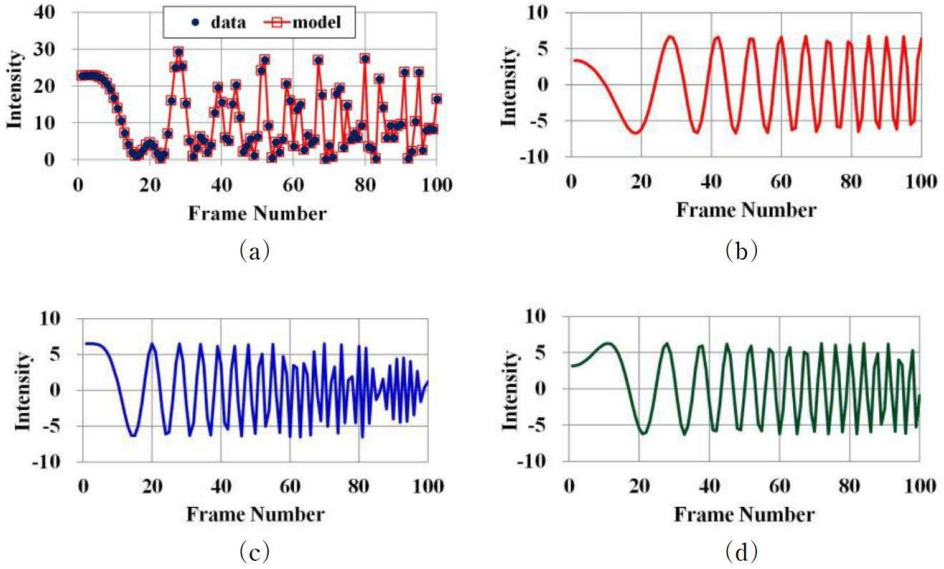

Fig.5 Results of simulated interferograms. (a) Simulated superimposed interferogram, (b) Separated interferogram between Ref-FS, (c) Separated interferogram between Ref-BS, (d) Separated interferogram between FS-BS.

Table 1 Estimation results

Variable	True	Estimated	Error
I_0	100	100.00	0.00
ϕ_{S0} (rad)	2.09	2.09	0.00
ϕ_{B0} (rad)	0.00	0.00	0.00

4. Actual experiment

4.1 Experimental method

We constructed the Fizeau interferometer shown in Fig. 1. The target sample is a glass plate (refractive index: 1.50, size: 125 × 125 mm, thickness 10 mm) with a convex surface on one side and a concave surface on the other side. It was installed at the distance of 18.8 mm from the reference . The field of view of the interferometer is about 300 mmφ, and the refractive index of the reference surface is 1.54. A wavelength-tunable laser diode (LD) with temperature control was adopted as the light source.

The center wavelength of this LD is 634 nm, and the wavelength change due to temperature control is about 0.04 nm/K. The temperature can be controlled by the analog voltage signal from the PC, and the wavelength can be shifted up to 0.5 nm.

The wavemeter is a commercial product based on the principle of an interferometer, has a nominal accuracy of 0.7 pm, and is connected to a PC via a USB interface.

The camera was 1360 x 1024 pixels, monochrome 8bit, 12 fps, and was connected to a PC via a USB interface.

Figure 6 shows the interference image at the initial wavelength obtained in this experiment. The central rectangular area (394 × 394 pixels; equivalent to 115 mm square) was used as the measurement area. The LD temperature was changed stepwise from 18.0°C (wavelength about 634.09 nm) to 24.3°C (wavelength about 634.31 nm), 128 wavelength shifts were performed, and images were captured. The estimated values used for the phase shift calculation were S_0＝18.8 mm and T_0 =10.0 mm. When the LD wavelength is shifted, the LD output also changes. This effect was compensated by using the fact that the LD wavelength and output are in a linear relationship, and obtaining the relationship from the measured average intensity.

We implemented the proposed algorithm on a Windows PC using C language. The calculation flow is as follows:

(1) Convert wavelength shift amount to phase shift amount.
(2) Compensation of LD output change.
(3) Phase estimation by the least-squares fitting at each pixel in the image.
(4) Phase unwrapping.
(5) Conversion phases to actual heights.

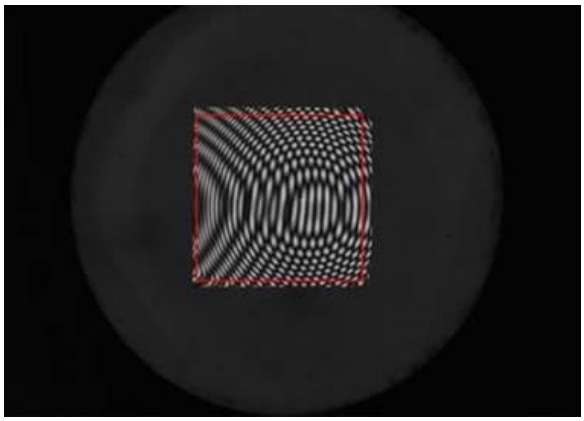

Fig.6 Measurement area of interference image

Although many methods have been proposed for phase unwrapping [27], the authors adopted a unique algorithm based on the neighborhood connection method. In addition, the measured values obtained are relative values, and the following post-processing calculation was added to remove the sample inclination.

(1) Front/back surface height: Converted to deviation from the best fitting plane.

(2) Thickness: Converted to deviation from the average value over the entire surface.

4.2 Experimental results

The measured wavelength and its linearity error are shown in Fig. 7(a). The initial wavelength was 634.095 nm, the final wavelength was 634.307 nm, the total wavelength shift was 0.212 nm, and the average wavelength shift per cycle was 1.66 pm. Also, a linearity error of about ±5 pm was observed. Howeve, this proposed method does not pose any problem because it assumes an arbitrary wavelength.

The interferogram at the coordinate origin is shown in Fig. 7(b). The intensity gradually decreases due to the influence of the LD output change. Figure 7(c) is a plot with the horizontal axis representing wavelength and the vertical axis representing the itensity value at the origin and the average intensity value at all points. From the regression coefficient a = -141.19 and the intercept b = 89601 of the regression line, the output change rate (a/b) = -0.1576% per unit wavelength (nm) can be obtained. The results of intensity correction using this rate of change are shown in Fig. 7(d). The LD output fluctuation is corrected and the average intensity value of each image is almost constant.

The corrected intensity data and the fitted model waveform are shown in Fig. 7(e). The results of phase estimation on the entire surface are shown in Figs. 8(b)(c)(d). It can be seen that the superimposed striped image in Fig. 8(a) is separated into three striped images. Figure 9 shows the height/plate thickness estimation results obtained from these phase distributions through unwrapping and data post-processing. Figure 10 shows the horizontal line profile along the the center point. The front surface height was convex, the back surface was concave, and the plate thickness was inclined.

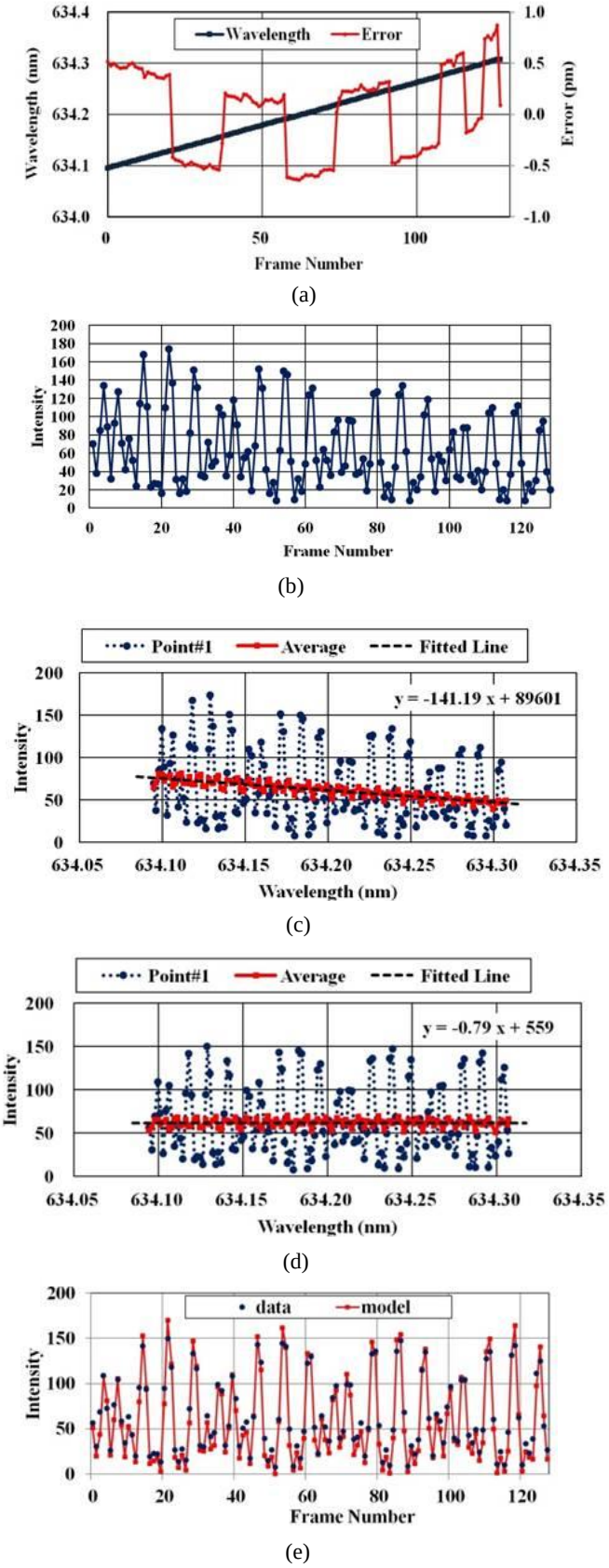

Fig.7 Experimental results. (a) Measured wavelength, (b) Interferogram at the center point, (c) Interferogram before intensity compensation, (d) Interferogram after intensity compensation, (e) Interferogram with its best-fit model.

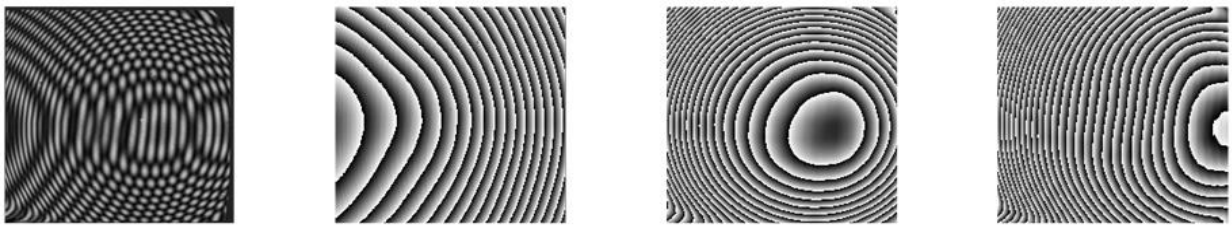

(a) (b) (c) (d)

Fig. 8 Interference image and estimated phases. (a) Original image, (b) phase of front surface, (c) phase of back surface, (d) phase of thickness.

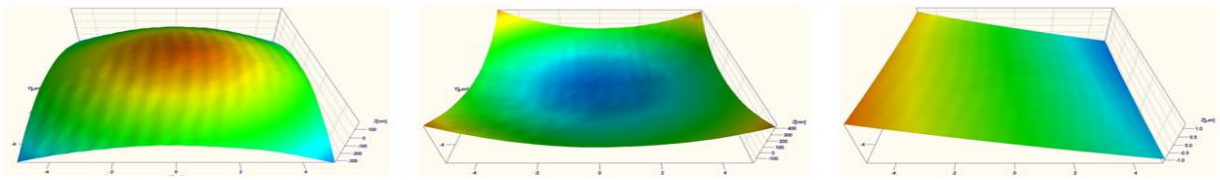

(a) (b) (c)

Fig.9 Measured 3D profiles. (a) Front surface, (b) back surface, (c) thickness.

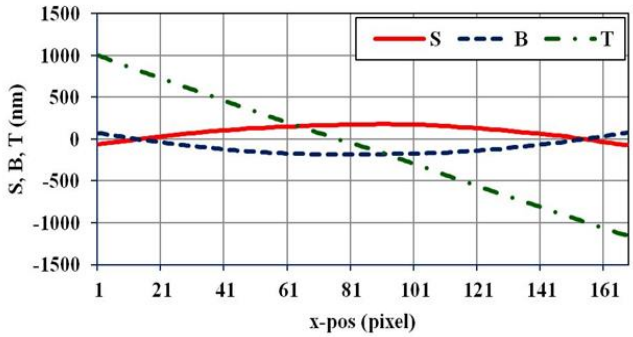

Fig.10 Estimated horizontal line profiles at the center position.

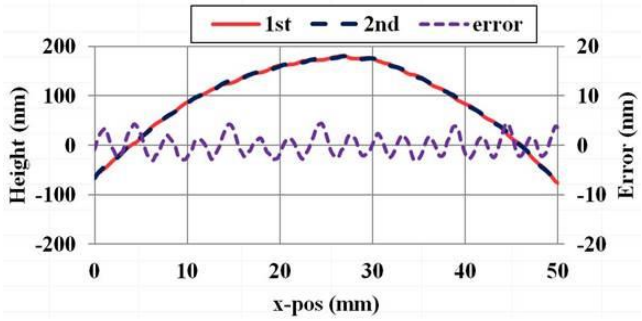

Fig.12 Repeatability evaluated by front surface profile measurements.

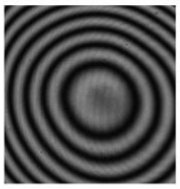

(a) Surface interference image

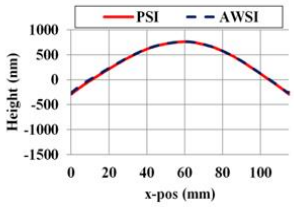

(b) Surface profiles

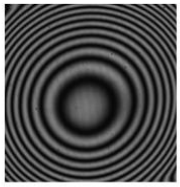

(c) Back surface interference image

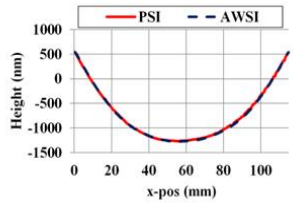

(d) Back surface profiles

Fig.11 Comparison between results of PSI and AWSI methods

In order to verify this result, antireflection treatment was applied to the back surface of the sample, and the surface profile was measured by the ordinary phase shift method (PSI method) using the fine piezo mechanism. The conditions for the PSI method are: shift amount = 90°; shift counts = 5 times. The results are shown in Fig. 11. Fig. 11(a) is the interference image when the front surface side is measured, and Fig. 11(b) is the line profile of the measurement results. In addition, Fig. 11(c) and (d) are the image and the results when the back side was measured. In Fig. 11(b) and (d), the measurement results of the PSI method shown by the dotted line and the proposed method (AWSI) shown by the solid line are in good agreement.

Next, Fig. 12 shows the results of the measurement reproducibility evaluation test. This shows the surface profile line profile obtained by two measurements and the difference between them, and the RMS reproducibility (σ) was 2.0 nm.

The measurement time is the sum of the image acquisition time and the calculation time. Since the former has a waiting time of 1 s for each shift, it is 128 s for 128 wavelength shifts, and the latter was about 3 s using a commercially available Windows PC (CPU: Core i7 6700K, 4GHz). It has been confirmed that there is a sufficient possibility of shortening these times, and that the number of shifts can be reduced to 32 times by allowing measurement value fluctuations of several nm, for example.

5. Conclusion

A new method was developed that allows the arbitrary wavelength shift without the need for highly accurate linear wavelength scanning in the simultaneous measurement of the surface profile, the back surface profile, and the plate thickness distribution of transparent plates by Fizeau interferometer and wavelength shift interferometry (AWSI method). In this method, the wavelength of the laser is measured by an external wavelength meter, and the obtained wavelength shift amount is converted into the phase shift amount. Next, the obtained phase shift amount and observed intensity values are least-squares-fitted to the interference signal model of the phase shift method to obtain the phases.

In order to stabilize this solution (i.e. to avoid the local minima problem) and speed up, the number of unknown variables was reduced to three which is the theoretical lower limit by assuming that the refraction indices of the reference surface and the sample are known. In order to speed up the calculation, the nonlinear least squares problem was linearized by variable transform.

The validity of the proposed method was confirmed by computer experiments and actual experiments. The surface profile measurement results of the uneven glass plate with a thickness of 10 mm were similar to those of the conventional phase shifting method measured with antireflection treatment on the back surface. The measurement reproducibility (RMS) was 2.0 nm. The analysis time is very fast, 3 s in the case of a measurement area of 394 × 394 pixels.

This method does not require highly accurate wavelength scanning, and a commercially available wavelength tunable LD light source can be used to realize a practical measuring device at a relatively low cost.

Supplement 1: Effect of estimated value error

In Section 2.1, the estimated value S_0 of the unknown variable S is used to obtain the phase shift amount from the wavelength shift amount, and it is assumed that the estimation error is sufficiently small. Here, the effect of the estimation error is analyzed focusing on the unknown variable S. That is, the effect of the estimation error ε_S on the estimation of the phase ϕ_{S0} is analyzed.

(1) Theoretical analysis

If the estimated value S_0 contains the estimation error ε_S,

$$S_0 = S+\varepsilon_S \tag{1-1}$$

The phase shift amount $\Delta\phi'_{Si}$ is calculated from Eqs. (12) and (1-1).

$$\begin{aligned}\Delta\phi'_{Si} &= -4\pi(S+\varepsilon_S)(\Delta\lambda_i)/\lambda_i\lambda_0 \\ &= \Delta\phi_{Si} - 4\pi\varepsilon_S(\Delta\lambda_i)/\lambda_i\lambda_0\end{aligned} \tag{1-2}$$

The second term on the right side of this equation is the phase shift error,

$$\delta\phi_{Si} = -4\pi\varepsilon_S(\Delta\lambda_i)/\lambda_i\lambda_0 \tag{1-3}$$

This shows that the error is proportional to ε_S and $\Delta\lambda_i$, and does not depend on S.

At this time, assuming that the wavelength shift amount $\Delta\lambda_i$ changes linearly, the error $\delta\phi_{S0}$ of the phase estimation value ϕ_{S0} obtained by the least-squares fitting is given from the equation (15):

$$\delta\phi_{S0} = -\mathrm{avg}(\delta\phi_{Si}) \tag{1-4}$$

where avg() represents the average value of i = [1, m]. From Eqs. (1-3) and (1-4),

$$\begin{aligned}\delta\phi_{S0} &= (4\pi\varepsilon_S/\lambda_0)[\mathrm{avg}(\Delta\lambda_i/\lambda_i)] \\ &\cong (4\pi\varepsilon_S/\lambda_0)(\Delta\lambda_{imax}/2\lambda_0) \\ &= 2\pi\varepsilon_S\Delta\lambda_{imax}/\lambda_0^2\end{aligned} \tag{1-5}$$

where $\Delta\lambda_{imax}$ is the maximum wavelength shift.

When converted to actual size, the estimation error δS is expressed by the following equation.

$$\begin{aligned}\delta S &= (\Delta\phi_{S0}/2\pi)(\lambda_0/2) \\ &= (\Delta\lambda_{imax}/2\lambda_0)\varepsilon_S\end{aligned} \tag{1-6}$$

That is, it becomes $(\Delta\lambda_{imax}/2\lambda_0)$ times the estimation error. For example, under the conditions of the actual experiment, $\Delta\lambda_{imax}/2\lambda_0 \cong 0.2/(2*600) \cong 1/6000$, and if ε_S =100 μm, $\delta S \cong$ 16 nm.

(2) Computer experiment and discussion

We will verify the theoretical consideration results in the previous section through computer experiments. Under the experimental conditions in Section 3.1, when the estimation error of S is 100 μm, the phase error of S is 0.34 rad and the height estimation error is 16.3 nm, which is almost the same as the theoretical analysis result.

From the above results, we consider the effect of the error of the estimated value from a practical point of view. First, it can be reasonably assumed that S, B and T can be estimated with an accuracy of 100 μm using a normal measuring instrument such as a caliper. Then the estimation error is about 16 nm. Also, this estimation error does not depend on the coordinates on the image and takes almost the same value as expressed by Eq. (1-6). Therefore it is expected that this error will be significantly canceled during the post-processing (Section 4.1) of obtaining the deviation from the fitted plane or the average value.

Supplement 2: Linear Least Squares Solution

The specific solution of the linear least squares method in Section 2.1 is described below. Substituting Eq. (17) into Eq. (18) and setting the partial derivative of each unknown variable of *SSE* as zero, the following simultaneous equation of 7 unknown variables is obtained.

A・X=Y

where

$$\mathbf{A} = \begin{vmatrix} an & -b_s\Sigma C_{Si} & b_s\Sigma S_{Si} & b_B\Sigma C_{Bi} & -b_B\Sigma S_{Bi} & -b_T\Sigma C_{Ti} & b_T\Sigma S_{Ti} \\ a\Sigma C_{Si} & -b_s\Sigma C_{Si}^2 & b_s\Sigma S_{Si}C_{Si} & b_B\Sigma C_{Bi}C_{Si} & -b_B\Sigma S_{Bi}C_{Si} & -b_T\Sigma C_{Ti}C_{Si} & b_T\Sigma S_{Ti}C_{Si} \\ a\Sigma S_{Si} & -b_s\Sigma C_{Si}S_{Si} & b_s\Sigma S_{Si}^2 & b_B\Sigma C_{Bi}S_{Si} & -b_B\Sigma S_{Bi}S_{Si} & -b_T\Sigma C_{Ti}S_{Si} & b_T\Sigma S_{Ti}S_{Si} \\ a\Sigma C_{Bi} & -b_s\Sigma C_{Si}C_{Bi} & b_s\Sigma S_{Si}C_{Bi} & b_B\Sigma C_{Bi}^2 & -b_B\Sigma S_{Bi}C_{Bi} & -b_T\Sigma C_{Ti}C_{Bi} & b_T\Sigma S_{Ti}C_{Bi} \\ a\Sigma S_{Bi} & -b_s\Sigma C_{Si}S_{Bi} & b_s\Sigma S_{Si}S_{Bi} & b_B\Sigma C_{Bi}S_{Bi} & -b_B\Sigma S_{Bi}^2 & -b_T\Sigma C_{Ti}S_{Bi} & b_T\Sigma S_{Ti}S_{Bi} \\ a\Sigma C_{Ti} & -b_s\Sigma C_{Si}C_{Ti} & b_s\Sigma S_{Si}C_{Ti} & b_B\Sigma C_{Bi}C_{Ti} & -b_B\Sigma S_{Bi}C_{Ti} & -b_T\Sigma C_{Ti}^2 & b_T\Sigma S_{Ti}C_{Ti} \\ a\Sigma S_{Ti} & -b_s\Sigma C_{Si}S_{Ti} & b_s\Sigma S_{Si}S_{Ti} & b_B\Sigma C_{Bi}S_{Ti} & -b_B\Sigma S_{Bi}S_{Ti} & -b_T\Sigma C_{Ti}S_{Ti} & b_T\Sigma S_{Ti}^2 \end{vmatrix} \tag{2-1}$$

$$\mathbf{X} = \begin{vmatrix} I_0 \\ C_S \\ S_S \\ C_B \\ S_B \\ C_T \\ S_T \end{vmatrix} \tag{2-2}$$

$$\mathbf{Y} = \begin{vmatrix} \Sigma I_i \\ \Sigma I_i C_{Si} \\ \Sigma I_i S_{Si} \\ \Sigma I_i C_{Bi} \\ \Sigma I_i S_{Bi} \\ \Sigma I_i C_{Ti} \\ \Sigma I_i S_{Ti} \end{vmatrix} \tag{2-3}$$

and Σ means the sum of (i = 1, m), $C_{Si} = \cos(\Delta\phi_{Si})$, $S_{Si} = \sin(\Delta\phi_{Si})$, $C_{Bi} = \cos(\Delta\phi_{Bi})$, $S_{Bi} = \sin(\Delta\phi_{Bi})$, $C_{Ti} = \cos(\Delta\phi_{Ti})$, $S_{Ti} = \sin(\Delta\phi_{Ti})$.

In the actual experiment, this linear equation was solved by the Gaussian elimination method.

Acknowledgment

We would like to thank Mr. Yoshihiro Miyamoto of Mizojiri Optical Co., Ltd. for contributing to the experimental system construction and the actual experiments in this research.

References

[1] Y. Ishii: Kogaku, **17** (1988) 295-296 (in Japanese).
[2] Y. Ishii and R. Onodera: J. Jpn. Soc. Precis. Eng., 64, 9 (1998) 1294-1298 (in Japanese).
[3] J. Schmit, K. Creath and J. C. Wyant: "Wavelength scanning interferometer," Optical Shop Testing, 3rd Ed., D. Malacara ed., (John Wiley & Sons, Inc., New York, 2007) .724-731.
[4] K. Hobino: Kogaku, **37** (2008) 564-569 (in Japanese).
[5] K. Okada, H. Sakuta, A. Sato and J. Tsujiuchi: Proceedings of Meeting on Lightwave Sensing Technology, (1990) 161-167 (in Japanese).
[6] K. Okada, H. Sakuta, T. Ose and J. Tsujiuchi: Appl. Opt., **29** (1990) 3280-3285.
[7] K. Kitagawa and J. Mizojiri: Proc. of JSPE Autumn Meeting, (2015) 771-772 (in Japanese).
[8] P. de Groot: Appl. Opt., **39** (2000) 2658-2663.
[9] K. Hibino and T. Takatsuji: Opt. Rev., **9** (2002) 60-65.
[10] K. Hibino, B. F. Oreb, P.S. Fairman and J. Burke: Appl. Opt., **43** (2004) 1241-1249.
[11] K. Hibino, J. Burke, R. Hanayama and B. F. Oreb: Opt. Express, **12** (2004) 5579-5594.
[12] R. Hanayama, K. Hibino, J. Burke, B. F. Oreb, S. Warisawa and M. Mitsuishi: J. Jpn. Soc. Precis. Eng., **71** (2005) 579-583 (in Japanese).
[13] K. Hibino, Y. Kim, Y. Bitou, S. Ohsawa, N. Sugita and M. Mitsuishi: J. Jpn. Soc. Precis. Eng., **76** (2010) 243-248 (in Japanese).
[14] L. L. Deck: "Multiple surface phase-shifting interferometry," Proc. SPIE, **4451** (2001) .424-431.
[15] L. L. Deck: Appl. Opt., **42** (2003) 2354-2365.
[16] O. Sasaki, S. Hirakubo, S. Choi and T. Suzuki: Appl. Opt., **51** (2012) 2429-2435.
[17] F. Gao, H. Muhamedsalih and X. Jiang.: Opt. Express, **20** (2012) 21450-21456.
[18] K. Yuksel, M. Wuilpart, V. Moeyaert and P. Megret: "Optical frequency domain reflectometry: A review," 11th International Conference on Transparent Optical Networks (2009). 1-5.
[19] K. Iiyama, L. T. Wang and K. I. Hayashi: J. Lightwave Technol., **14** (1996) 173–178.
[20] E. Brinkmeyer and U. Glombitza: "High-resolution coherent frequency-domain reflectrometry using continuously tuned laser diodes," in Optical Fiber Communication, vol.4, OSA Technical Digest Series (Optical Society of America, 1991), paper WN2.
[21] R. Huber, M. Wojtkowski, K. Taira, J. G. Fujimoto and K. Hsu: Opt. Express, **13** (2005) 3513-3528.
[22] K. Okada, A. Sato and J. Tsujiuchi: Opt. Comm., **84** (1991) 118-124.
[23] G. S. Han and S. W. Kim: Appl. Opt., **33** (1994) 7321-7325.
[24] Z. Wang and B. Han: Opt. Lett., **29** (2004) 1671-1673.
[25] R. Juarez-Salazar, C. Robledo-Sánchez, C. Meneses-Fabian, F. Guerrero-Sánchez and L. A. Aguilar: Opt. Lasers Eng., **51** (2013) 626–632.
[26] K. Kitagawa and J. Mizojiri: Proc. of JSPE Autumn Meeting, (2016) 29-30 (in Japanese).
[27] D. C. Ghihlia and M. D. Pritt: Two-dimensional Phase Unwrapping: Theory, Algorithms, and Software, (John Wiley and Sons, Inc., New York, 1998).

This is an English translation of the paper:
Katsuichi Kitagawa and Jun Mizojiri: "Simultaneous Measurement of Transparent Plate Surface Topography and Thickness Variation using Arbitrary Wavelength Shifting Interferometry ", Kogaku, 47(4) 165-173 (2018) (original in Japanese; translated by the first author)